Int. J. Corros. Scale Inhib., 2017, **6**, no. 3, 307–317

SVET study of the interaction of 2-mercaptobenzothiazole corrosion inhibitor with Au, Cu and Au–Cu galvanic pair

J.A. Ramírez-Cano,[1] L. Veleva,[1]* B.M. Fernández-Pérez[2] and R.M. Souto[2]

[1]*Department of Applied Physics, Centre for Investigation and Advanced Studies (CINVESTAV), km. 6 Carr. Antigua a Progreso, AP 73, Cordemex, 97310 Merida, Yucatan, Mexico*

[2]*Department of Chemistry, Universidad de La Laguna, P.O. Box 456, 38200 La Laguna, Tenerife, Canary Islands, Spain*

**E-mail: veleva@cinvestav.mx*

Abstract

This study reports an electrochemical investigation of the interaction between 2-mercaptobenzothiazole (2MBT), a corrosion inhibitor, and two noble metals (Cu and Au), either isolated or under galvanical coupling. The surface reactivity of the inhibitor-modified metals in chloride-containing aqueous solution of 0.1 mM NaCl was studied using the Scanning Vibrating Electrode Technique (SVET). The potential gradients in the electrolyte were detected by the SVET and converted to local ionic currents distributed at different anodic and cathodic sites, where electrochemical redox reactions are taking place. No external polarization was applied during SVET measurements, leaving the samples at the spontaneous free corrosion potential (FCP). The values of FCP showed that the metals are not protected by 2MBT. SVET revealed a moderate electrochemical activity of Au and very low in the case of Cu.

Keywords: copper, gold, SVET, neutral inhibition, galvanic coupling.

Received: May 29, 2017. Published: June 24, 2017. doi: 10.17675/2305-6894-2017-6-3-6

1. Introduction

Corrosion is one of the biggest challenges causing massive economic losses that modern day electronic industry faces and has a major impact because of the high technological dependence of modern society. As a consequence, the study of effective methods to prevent corrosion has become a very important and interesting topic among researchers [1–4].

The use of organic corrosion inhibitors is one of the most effective and economic methods [5–10]. Most reports indicate that applied in very small concentrations, the organic inhibitors are capable of protecting metals from aggressive environments by adsorbing on the metal surface and creating a physical barrier [10–19]. Their adsorption takes place through heteroatoms like nitrogen, oxygen, sulphur, *etc*. Despite the widespread study and use of inhibitors, the adsorption configurations and electrochemical

processes that lead to corrosion inhibition remain unclear [20–24]. Among the organic compounds used as corrosion inhibitors, those belonging to the azole group are regarded as effective inhibitors [5, 12, 13, 25–29]. In particular, 2-mercaptobenzothiazole (2MBT) is considered a good corrosion inhibitor for copper [5, 14], being the second most efficient inhibitor for copper [30] among the azole family.

The scanning vibrating electrode technique (SVET) is a valuable microelectrochemical technique [31, 32] that has been employed previously to study metal–inhibitor systems [33–41]. Because corrosion inhibition is a very complex process, where corrosion inhibitors interact with corrosion cells in micrometer or even nanometer scales, *in situ* analysis in those dimensions are needed to obtain a comprehensive understanding of the inhibition mechanism. This is why SVET is a very useful technique to study corrosion inhibition processes. The enhanced local resolution of this technique enables the direct characterization of electrochemical processes involved in the corrosion phenomena. An electrochemical activity mapping allows assessment of the effect of adsorbed molecules on the ionic current distribution developed over the metallic sample, providing an insight about the relevant electrochemical processes during metal–inhibitor interaction.

In this work, the electrochemical interaction between 2-mercaptobenzothiazole and two noble metals, namely Au and Cu, was studied employing SVET, in order to assess the effect on the ionic current density distribution on inhibitor-modified metals during exposure in 1 mM NaCl solution. Given the close proximity between gold- and copper-made components in microelectronics, the Au–Cu galvanic pair is also of major interest. No external polarization was applied during SVET measurements, leaving the samples at the spontaneous free corrosion potential (FCP).

2. Experimental methods

2.1 Materials preparation

Reactant grade 2MBT, acquired from Aldrich with a purity of 97%, was employed. Twice distilled water (18.2 MΩ) was used to prepare aqueous solutions containing either 1 mM 2MBT for metal surface treatment, or 1 mM NaCl as test solution. For SVET measurements, Pt/Ir (80%/20%) probes with a length of 2–3 cm were used, coated with parelene C, except at the tip, so that only this end works as sensor. Two Pt wires are employed as reference electrodes. These Pt electrodes were platinized with the purpose of creating a spherical black platinum deposit of 10–20 μm of diameter. Electrochemical activity mapping was carried out in constant height mode with the probe at 100 μm from the surface. Tip vibration was performed perpendicularly to the sample surface with 50 μm amplitude (100 μm peak to peak amplitude).

Au, Cu and Au–Cu pair samples were prepared from Au and Cu wires of electrolytic grade (99.999%), with diameters of 500 and 125 μm, respectively. They were embedded in Epofix resin (Struers, Ballerup, Denmark), to expose their cross sections to the test

electrolyte (1 mM NaCl). The separation between wires is 1.8 mm, which is enough distance to avoid any eventual product formed on one metal to modify the local chemistry of the other for the duration of the experiments (60 min). When desired, electric contact between both metals in the Au–Cu pair could be established at the rear of the mold. A small container for the electrolyte was created using adhesive tape to surround the cylindrical epoxy mold.

2.2 Free corrosion potential measurements

Free corrosion potential (FCP) values of Au, Cu and the galvanic pair Au–Cu were monitored during 60 min in inhibitor-free and inhibitor-containing solutions, having inhibitor concentration of 1 mM. FCP values were recorded with an AUTOLAB (Metrohm, Herisau, Switzerland) bipotentiostat, controlled by a computer. The values presented here correspond to the average value for each system, and it was corrected considering the standard potential of the Ag/AgCl/KCl (3 M) reference electrode.

2.3 SVET: electrochemically-resolved surface activity

Prior to SVET mapping, the specimens were submerged during 60 min in inhibitor solution, then rinsed using ethanol, and taken to the SVET cell where the 1 mM NaCl solution is added. Because of the high sensitivity of electrochemical scanning techniques (such as SVET) it is recommended to operate in a test electrolyte of low ionic strength. Using a video camera, the vibrating probe is placed above the selected area for scanning. Since it is not possible to position the sample exactly in the same place for each experiment, the scan area was taken as to include the metal surface and a portion of the surrounding resin. Depending on the size of the sample, the scanned area can be up to 1500 μm by 2000 μm. Comparison between scans can be performed because the area difference between experiments is negligible. The recording of a single map lasts 6 min, hence a total of 10 scans lasted 60 min. In this manner, the spatial distribution of the surface activity is obtained and allows differentiating between local anodic and cathodic areas on the metal surface. The resulting activity surfaces are plotted using a custom-made program built in MATLAB that allows the acquisition of isometric and XY-plane graphics.

3. Results and discussion

3.1 Free corrosion potential analysis

FCP measurements were conducted at open circuit in order to investigate the effect of 2MBT inhibitor film, adsorbed on the surface of metals, on their corrosion resistance in a test aqueous electrolyte solution. The FCP average values are shown in Table 1.

Table 1. [mV *vs* NHE] Mean FCP values recorded of Au–Cu, Au and Cu after 1 h of immersion in 1 mM NaCl (inhibitor free) and in 1 mM 2MBT aqueous solutions.

Metal specimen	FCP [mV *vs*. NHE]	
	in 1 mM NaCl	in 1 mM 2MBT
Au–Cu	–437.2	–459.6
Au	–149.5	–207.2
Cu	–286.4	–417.4

FCP values indicate that the 2MBT adsorbed film has a negative effect on the corrosion resistance of both metals and their galvanic coupling, shifting the FCP of the metals to more negative values. Namely, in the case of Au–Cu the shift was ΔFCP = –22.4 mV, for the Au specimen was ΔFCP = –57.7 mV, and for Cu was ΔFCP = –131 mV. It is interesting to observe that the biggest change in FCP has occurred for copper, though 2MBT is considered to be a good corrosion inhibitor for copper [5, 25, 26, 42], and we would expect a shift toward more positive FCP values in 2MBT treated Cu.

3.2 Electrochemical reactivity imaging by SVET

SVET was employed to characterize variations in surface reactivity of the metals due to the presence of an adsorbed inhibitor film on their surface while submerged in 1 mM NaCl solution. Potential differences in the electrolyte arise naturally from distributed electrochemical activities on either bare or inhibitor-treated surfaces, originating local ionic currents in the electrolyte volume close to the metal samples. Potential gradients in the electrolyte are detected by the vibrating reference electrode and the gradients can be converted to local ionic currents by considering solution conductivity [31].

In this way, ionic current distributions at different locations on the surface can be associated with experimental features where an electrochemical redox conversion is taking place. Anodic sites on the surface correspond to positive ionic currents, while cathodic sites are associated with negative ionic currents. No external polarization was applied during SVET measurements, leaving the samples at either the spontaneous FCP of each metal, or at the mixed potential in the case of the Au-Cu galvanic pair.

3.2.1 Surface reactivity of Au pretreated with 2MBT

The ionic current density maps of the Au–2MBT system are presented in Figure 1. During the first 6 min of the scan (Figure 1a), it is possible to distinguish the approximate location of the gold surface (500 μm dia.) due to the localized occurrence of high positive ionic currents over this metal. The ionic current density range covered in this activity map extends from –1.75 to 20 μA cm^{-2}, wider than the corresponding ionic current density

range monitored for pristine Au immersed in 1 mM NaCl test (*i.e.*, from –0.4 to 0.4 μA cm^{-2}, not shown). Though the gold wire is located approximately at the center of the scanned area, its actual shape is not distinguishable from the surrounding epoxy resin, a fact that can be attributed to the low reactivity of gold in 1 mM NaCl solution. Given that 2MBT is a tautomer, the observation of a positive ionic current in the system must be attributed to the deprotonation of 2MBT molecule [42] during its tautomeric equilibrium. Furthermore, the possible formation of a multilayer structure on gold during the pretreatment step in 2MBT solution, would lead to greater instability in the outermost molecules adsorbed on gold when the organic compound is not present in the test solution. These molecules could detach and, once in aqueous solution, resume their tautomeric equilibrium deprotonating and appearing in the SVET scan as an apparent anodic activity (*i.e.*, positive ionic currents). As these detached molecules spread in the bulk of the solution, we will lose the initial surface resolution, because there is no more localized deprotonation over Au. This will lead to the homogenization of the electrochemical activity and the decrease of the ionic current density ranges for the SVET maps recorded at longer times (see Figure 1b and 1c), although after 60 min it exhibits some residual activity that accounts for a bigger current range than for pristine Au.

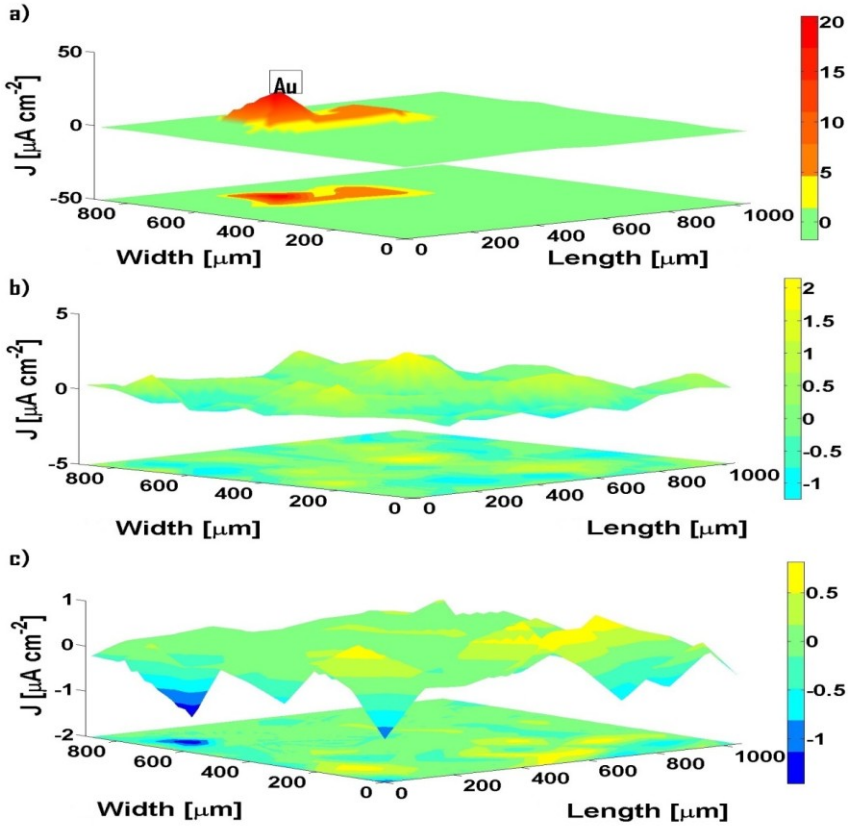

Figure 1. Ionic current density distributions over 2MBT-modified Au in 1 mM NaCl at various immersion times: (a) 6, (b) 30, and (c) 60 min.

The FCP values for this system (Table 1) also indicate that 2MBT has a negative effect on Au, shifting the FCP to more negative values. However, this result can be explained by the tautomeric equilibrium described above. In this way, 2MBT will act as a multi-mechanism inhibitor, forming a multilayer physical barrier and also interacting with the electrolyte by detaching the outermost molecules and probably forming compounds with the electroactive species present in solution.

3.2.2 Surface reactivity of Cu pretreated with 2MBT

Pristine Cu immersed in 1 mM NaCl solution exhibits a very similar behaviour to non-treated gold, characterized by a featureless distribution involving very low ionic current densities ranging between –0.5 and 0.3 μA cm^{-2}. In consequence, the shape of the copper surface is undistinguishable from the surrounding resin.

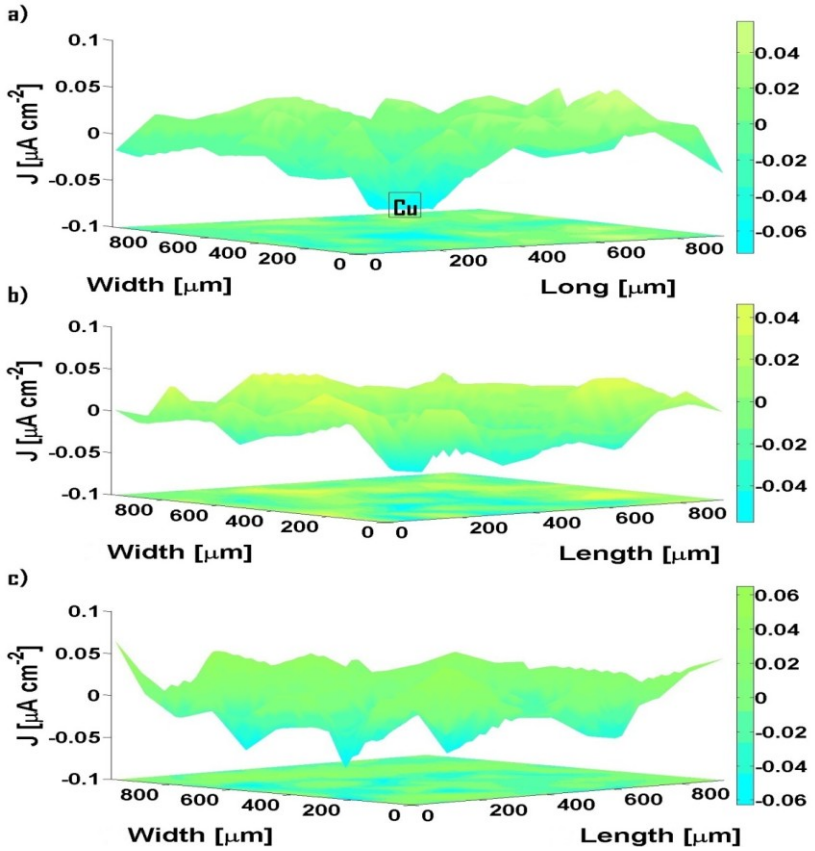

Figure 2. Ionic current density distributions over 2MBT-modified Cu in 1 mM NaCl at various immersion times: (a) 6 , (b) 30, and (c) 60 min.

The SVET imaging of the Cu-2MBT system is presented in Figure 2, with a maximum current density range between –0.06 μA cm^{-2} and 0.06 μA cm^{-2}. Despite the fact that ionic current density is within the background noise, the location of the Cu surface treated with 2MBT is slightly distinguishable in the first 6 min (*cf.* Figure 2a) and

subsequently disappears. Considering that the electrode diameter is 125 μm, the weak electrochemical activity observed at 30 min (Figure 2b) is actually located outside the area of the electrode. The ability to resolve Cu surface could be due to the presence of adsorbed 2MBT on Cu that is electrochemically interacting with the electrolyte.

It is worth noticing, that the current density range for the treated sample is considerably lower than the one found in the non-treated sample, since after 30 min falls within the base zero color used in the color map. At this point, the current density range is one order of magnitude smaller and remains, basically, unvaried for the rest of the experiment. This result supports the idea that the FCP displacement to more negative values only corresponds to the protonation/deprotonation process that takes place in the tautomeric equilibrium of 2MBT in aqueous solution and not the metal being attacked by the inhibitor.

The adsorption energy and frequency variation of 2MBT on Cu [17] is lower than 2MBT on Au [16] as it was expected since thiazole compounds have high affinity for gold. Therefore, 2MBT molecules will find more suitable adsorption sites on Au than on Cu, giving place to a denser and thicker film. The higher adsorption energy also adds stability to the film, favoring the formation of a multilayer structure on Au that can survive the ethanol rinsing previous to SVET measurement, while Cu may not be capable to provide a good substrate for the formation of a stable multilayer 2MBT film. As result, 2MBT molecules adsorbed on Cu will have a much weaker bond with the metal surface, resulting in more molecules capable of resuming their tautomeric equilibrium once in aqueous NaCl solution and therefore, we cannot observe the positive ionic currents present in 2MBT treated Au. Next, the FCP value of the 2MBT–Cu system is considerably more negative than the NaCl–Cu and 2MBT–Au systems, and this could be due to the presence of a higher number of 2MBT molecules in the bulk of the solution, given that Cu is not capable to adsorb as many molecules as Au. In this way, the amount of molecules protonating and deprotonating in the 2MBT–Cu system is considerably higher and gets translated as a more negative FCP value.

3.2.3 Surface reactivity of Au–Cu galvanic pair pretreated with 2MBT

The Au–Cu galvanic pair was investigated next. In this case, the electric connection between the Au and Cu wires in the sample was established at the rear of the mould. The SVET response of this system has already been described somewhere else [43]. In brief, due to the electrical coupling between both metals, Cu acts as the anode of the system and Au as the cathode, thus making possible both metals to be well resolved from the surrounding resin in the ionic current density maps. The ionic current range extended from -2 μA cm^{-2} to 2 μA cm^{-2}.

A rather different situation is found in the ionic current density maps of the Au–Cu galvanic pair treated with 2MBT, as shown in Figure 3. Firstly, the presence of 2MBT on the surface of the metals greatly decreases the ionic current density range, setting the

anodic maximum at 0.55 μA cm^{-2} and the cathodic maximum at −0.53 μA cm^{-2}. Secondly, it is impossible to resolve the metallic surfaces at the end of the experiment (*cf*. Figure 3c). Thus, though it still possible to partially resolve the Cu surface at the beginning of the experiment (see Figure 3a), the signals monitored after 30 min immersion corresponds exclusively to background noise, which renders the resolution of both metallic surfaces impossible.

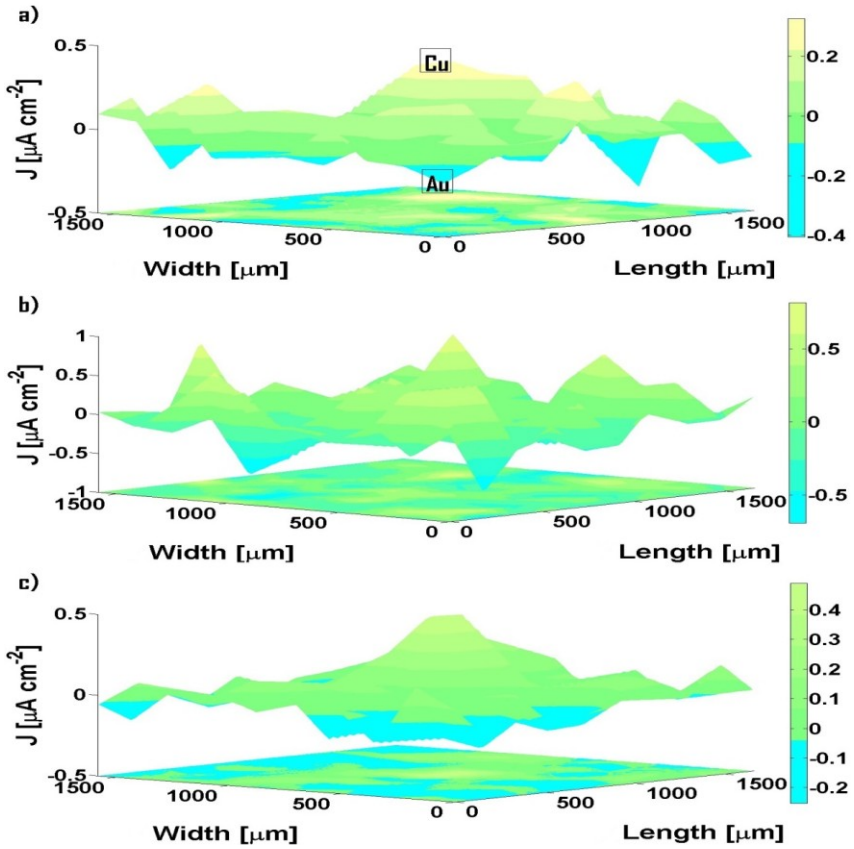

Figure 3. Ionic current density distributions over 2MBT-modified Au–Cu galvanic pair in 1 mM NaCl at various immersion times: (a) 6, (b) 30, and (c) 60 min (c).

The electrochemical activity (current density range) observed in the treated Au–Cu pair is thus rather similar to that already described for the non-treated Cu and Au samples. As discussed before, in the case of Au it is due to the low reactivity in NaCl solution, whereas in the case of Cu is probably because of the formation of an insulating corrosion product layer. Because of the electric coupling between both metals, Au is forced to act as cathode, while Cu behaves as the anode.

It must be noticed that Cu initially showed electrochemical activity as it was exclusively an anode, but subsequently reduced its electrochemical activity to almost zero in less than 1 hour. It has been reported in the literature that a film of 2MBT can be adsorbed on copper corrosion layers (Cu_2O and CuO) [42]. So, the sudden drop of

electrochemical activity observed over Cu, could be due to 2MBT molecules being desorbed and resuming their tautomeric equilibrium in a very similar fashion to what is observed in the case of Au treated with 2MBT. The presence of 2MBT makes the FCP of the Au–Cu pair more negative (Table 1), given that the adsorption of this compound corresponds to a physisorption process [17].

4. Conclusions

The presence of 2MBT on Cu and Au samples modifies their free corrosion potential value: in the case of Au it is shifted to more negative values by ΔFCP = –57.7 mV, while Cu becomes considerably more negative with ΔFCP = –131 mV. At the light of the FCP values it might be considered that this compound is not an efficient corrosion inhibitor for Cu. However, the current density maps obtained by SVET show that there is a significant reduction in the ionic current density range for Cu in the presence of 2MBT, while Au presents an increase in current density, a feature attributed to the tautomeric equilibrium of 2MBT. When the galvanic Au–Cu pair was treated with 2MBT, a considerable decrease in the current density range was observed. On the basis of the results reported in this work, we can conclude that SVET is a valuable electrochemical tool that allows the more precise characterization of inhibitor–metal interaction. In this way SVET scans showed 2MBT is capable of significantly reducing the ionic current density range related to electrochemical reactivity of Cu and Au–Cu samples in 1 mM NaCl solution when they were treated with this organic compound.

Acknowledgments

The authors would like to express their gratitude to the National Council of Science and Technology of México (CONACYT), for the scholarship no. 290936 granted to J.A. Ramírez-Cano to carry out a research stay at the Universidad de La Laguna (Spain).

References

1. X.G. Li, D.W. Zhang, Z.Y. Liu, Z. Li, C.W. Du and C.F. Dong, *Nature*, 2015, **527**, 441.
2. A. Cook, G. Frankel, A. Davenport, T. Hughes, S. Gibbon, D. Williams, H. Bluhm, V. Maurice, S. Lyth, P. Marcus, D. Shoesmith, C. Wren, J. Wharton, G. Hunt, S. Lyon, T. Majchrowski, R. Lindsay, G. Williams, B.R. Oller, M. Todorova, S. Nixon, S.T. Cheng, J. Scully, A. Wilson, F. Renner, Y.H. Chen, C. Taylor, H. Habazaki, A. Michaelides, S. Morsch, P. Visser, L. Kyhl and A. Kokalj, *Faraday Discuss*., 2015, **180**, 543.
3. M.O. Abdulazeez, A.K. Oyebamiji and B. Semire, *Int. J. Corros. Scale Inhib.*, 2016, **5**, no. 3, 248. doi: 10.17675/2305-6894-2016-5-3-5

4. A. Brenna, F. Bolzoni, MP. Pedeferri and M. Ormellese, *Int. J. Corros. Scale Inhib.*, 2017, **6**, no. 1, 59. doi: 10.17675/2305-6894-2017-6-1-5
5. M.M. Antonijevic and M.B. Petrovic, *Int. J. Electrochem. Sci.*, 2008, **3**, 1.
6. N.K. Allam, A.A. Nazeer and E.A. Ashour, *J. Appl. Electrochem.*, 2009, **39**, 961.
7. Kh. Rahmani, R. Jadidian and S. Haghtalab, *Desalination*, 2016, **393**, 174.
8. P.B. Raja, M. Ismail, S. Ghoreishiamiri, J. Mirza, M.C. Ismail, S. Kakooei and A.A. Rahim, *Chem. Eng. Commun.*, 2016, **203**, 1145.
9. K. Xhanari and M. Finšgar, *Arab. J. Chem.*, 2016, Article in Press. doi: 10.1016/j.arabjc.2016.08.009
10. I.A. Arkhipushkin, Yu.E. Pronin, S.S. Vesely and L.P. Kazansky, *Int. J. Corros. Scale Inhib.*, 2014, **3**, no. 2, 78. doi: 10.17675/2305-6894-2014-3-2-078-088
11. J. Telegdi, A. Shaban and E. Kálmán, *Electrochim. Acta*, 2000, **45**, 3639.
12. R. Subramanian and V. Lakshminarayanan, *Corros. Sci.*, 2002, **44**, 535.
13. E. Cano, J.L. Polo, A. La Iglesia and J.M. Bastidas, *Adsorption*, 2004, **10**, 219.
14. M.M. Antonijević, S.M. Milić and M. B. Petrović, *Corros. Sci.*, 2009, **51**, 1228.
15. M. Finšgar, *Corros. Sci.*, 2013, **77**, 350.
16. J.A. Ramírez-Cano and L. Veleva, *Solid State Phenom.*, 2015, **227**, 99.
17. J.A. Ramírez-Cano and L. Veleva, *Rev. Metal. (Madrid, Spain)*, 2016, **52**, 064, URL: http://revistademetalurgia.revistas.csic.es/index.php/revistademetalurgia/article/view/1377, doi: 10.3989/revmetalm.064
18. Yu.I. Kuznetsov, *Int. J. Corros. Scale Inhib.*, 2015, **4**, no. 1, 15. doi: 10.17675/2305-6894-2015-4-1-015-034
19. Yu. I. Kuznetsov, *Int. J. Corros. Scale Inhib.*, 2015, **4**, no. 4, 284. doi: 10.17675/2305-6894-2015-4-4-1
20. G. Trabanelli and V. Carassiti, in *Advances in Corrosion Science and Technology,* Eds. M.G. Fontana and R. W. Staehle, Plenum Press, New York, NY, 1970, p. 147.
21. D. Chadwick and T. Hashemi, *Surf. Sci.*, 1979, **89**, 649.
22. J. Zhang, Q. Zhang, H. Ren, W. Zhao and H. Zhang, *Appl. Surf. Sci.*, 2007, **253**, 7416.
23. P. Morales-Gil, M.S. Walczack, R.A. Cottis, J.M. Romero and R. Lindsay, *Corros. Sci.*, 2014, **85**, 109.
24. L. Guo, I.B. Obot, X. Zheng, X. Shen, Y. Qiang, S. Kaya and C. Kaya, *Appl. Surf. Sci.*, 2017, **406**, 301.
25. J.C. Marconato, L.O. Bulhões and M.L. Temperini, *Electrochim. Acta*, 1998, **43**, 771.
26. M. Finšgar and D.K. Merl, *Corros. Sci.*, 2014, **83**, 164.
27. D.A. Winkler, M. Breedon, A.E. Hughes, F.R. Burden, A.S. Barnard, T.G. Harvey and I. Cole, *Green Chem.*, 2014, **16**, 3349.
28. E.A. Skrypnikova, S.A. Kaluzhina and L.E. Agafonova, *Int. J. Corros. Scale Inhib.*, 2014, **3**, no. 1, 59. doi: 10.17675/2305-6894-2014-3-1-059-065
29. A. Shaban, Gy. Vastag and L. Nyikos, *Int. J. Corros. Scale Inhib.*, 2015, **4**, no. 4, 328. doi: 10.17675/2305-6894-2015-4-4-3

30. V. Lakshminarayanan, R. Kannan and S.R. Rajagopalan, *J. Electroanal. Chem.*, 1994, **364**, 79.
31. R.S. Lillard, in *Analytical Methods in Corrosion Science and Engineering,* Eds. P. Marcus and F. Mansfeld, CRC Press, Boca Raton, FL, 2005, p. 571.
32. S. Rossi, M. Fedel, F. Deflorian and M.C. Vadillo, *C. R. Chimie*, 2008, **11**, 984.
33. M.J. Franklin, D.C. White and H. S. Isaacs, *Corros. Sci.*, 1992, **33**, 251.
34. F. Thébault, B. Vuillemin, R. Oltra, K. Ogle and C. Allely, *Electrochim. Acta*, 2008, **53**, 5226.
35. M. Reffass, R. Sabot, M. Jeannin, C. Berziou and Ph. Refait, *Electrochim. Acta*, 2009, **54**, 4389.
36. G. Williams, H.N. McMurray and R. Grace, *Electrochim. Acta*, 2010, **55**, 7824.
37. A.M. Simões and J.C.S. Fernandes, *Prog. Org. Coat.*, 2010, **69**, 219.
38. S. Kallip, A.C. Bastos, M.L. Zheludkevich and M.G.S. Ferreira, *Corros. Sci.*, 2010, **52**, 3146.
39. M. Taryba, S.V. Lamaka, D. Snihirova, M.G.S. Ferreira, M.F. Montemor, W.K. Wijting, S. Toews and G. Grundmeier, *Electrochim. Acta*, 2011, **56**, 4475.
40. J. Izquierdo, J.J. Santana, S. González and R.M. Souto, *Prog. Org. Coat.*, 2012, **74**, 526.
41. L.B. Coelho, M. Mouanga, M.E. Druart, I. Recloux, D. Cossement and M.G. Olivier, *Corros. Sci.*, 2016, **110**, 143.
42. M. Ohsawa and W. Süetaka, *Corros. Sci.*, 1979, **19**, 709.
43. J.A. Ramírez-Cano, L. Veleva, R.M. Souto and B.M. Fernández-Pérez, *Mater. Corros.*, in press.

♦ ♦ ♦